Progress In Electromagnetics Research C, Vol. 88, 133–143, 2018

Numerical Study of a Photonic Jet with Aperiodic Fourier Modal Method and Experimental Validation

Hishem Hyani[1, 2, *], Bruno Sauviac[1], Kofi Edee[2], Gerard Granet[2], and Stephane Robert[1]

Abstract—This paper proposes to use an Aperiodic Fourier Modal Method (A-FMM) to model an outgoing photonic jet from a dielectric loaded waveguide ended by a tip with a specific shape. The proposed method has several advantages. First of all, the method is fast, which allows to manage optimization investigations. Secondly, the study of excitation (and more particularly the impact of plane wave excitation) can be examined precisely. Using our modelling technique, we show, in comparison with an actual optimized elliptical tip, that an optimized rectangular tip improves energy concentration by 8% and reduces the calculation time by a factor of 10. Furthermore, A-FMM allows to show that plane wave excitation modifies the spatial distribution of the jet, especially in the case of TE polarization. This can explain the differences observed, in previous works, where only fundamental mode excitation was used in the modelling. To validate these general results, prototypes have been realized, and measurements in the microwave regime have been compared favorably with simulation results.

1. INTRODUCTION

Intuitively, when the light interacts with a dielectric whose size is equal to a few wavelengths, a diffusion phenomenon is observable. But in 2004, Chen et al. [1] showed a new phenomenon. They observed a near-field focusing, weakly divergent with the full-width at half-maximum (FWHM) that could be smaller than the wavelength. So, this high-intensity beam can overtake the classical diffraction limit. This finding of considerable scientific importance has been successfully used for several applications. For instance, Chen et al. [1] showed an enhancement of the back-scattering of visible light by nanoparticles. Then Kong et al. [2, 3] used sub-wavelength beam to improve optical data-storage devices. This phenomenon can be obtained by cylinders [1], spheres [4, 5] or by micro cuboids [6].

Currently, the generation of photonic jets is mainly carried out with a free space excitation. However, some works use surface plasmon polaritons to excite a micro-scaled dielectric of different shapes [7, 8]. Photonic jets can also be produced using waveguide structures as done in [9–12]. In these works, modelling is done with an integral method [10]. Experimental validations are made at microwave frequencies [13]. Nevertheless, in the experimental setup, a plane wave is used to excite the waveguide.

In this paper, we propose to study the same guided structure as in the previously mentioned works (Fig. 1(a)) with a fast modal method. Our goal is to find a new shape of the tip that could achieve better focusing performance. Furthermore, we show that plane wave excitation modifies the electromagnetic distribution of the jet, especially in the case of TE polarization. This influence is more visible with a rectangular tip than with an elliptical tip.

The modelling is realized using an Aperiodic Fourier Modal Method (A-FMM) validated by numerical comparison with integral approach. Furthermore, the fastness of the method allows

Received 2 October 2018, Accepted 5 November 2018, Scheduled 16 November 2018

* Corresponding author: Hishem Hyani (hy.hishem@gmail.com).

[1] Univ Lyon, UJM-Saint-Etienne, CNRS, Laboratoire Hubert Curien, UMR5516, F42023, Saint-Étienne, France. [2] Institut Pascal, Université Clermont Auvergne, CNRS, UMR6602, 4 Avenue Blaise Pascal 63178 Aubiére, France.

optimization investigation. A very simple rectangular tip is found to be better than classical elliptic shape, in particular when we study the intensity. A prototype is realized and measured to validate our theoretical approach.

2. THEORY OF APERIODIC FMM

The Fourier modal method (FMM) or Rigorous Coupled-Wave Analysis (RCWA) is a technique which has been extensively used to solve electromagnetic problems, specifically diffraction gratings. This method was first proposed in 1978 by Knop [14].

Currently, the FMM is the most popular method for describing the interaction between electromagnetic waves and gratings. After a 20-year period with convergence problems, especially for interactions between metallic gratings and transverse magnetic field, Lalanne and Morris [15], and Granet and Guizal [16] solved the problem. They found a numerical solution by using two different convolution matrices associated with the permittivity function. In the same year, Li provided a mathematical justification and introduced the now well-known Fourier factorization rules [17].

Obviously, these methods are dedicated to periodic problems. Before studying the non-periodic structure, we will briefly present the FMM. The parallel plate waveguide ended by a tip is considered as the elementary cell of a grating, as illustrated in Fig. 1, where ε_1 is the relative permittivity of the dielectric and ε_2 the complex relative permittivity of the metal.

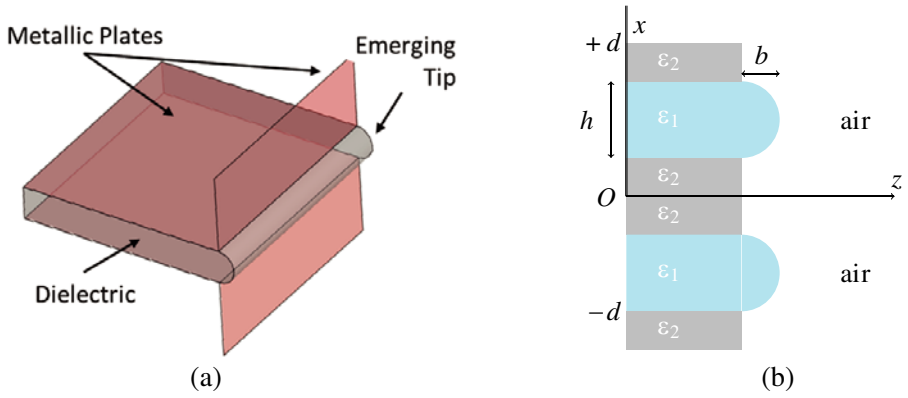

Figure 1. (a) Parallel plate waveguide under study (3D vision). (b) Periodical structure obtained using FMM (Side view of 2 elementary cells of the gratings).

This structure is invariant along the y-axis and is excited by the fundamental mode. The polarization can be either TE (the only non null components of the field are E_y, H_x and H_z) or TM (the only non null components of the field are E_z, E_x and H_y). It is well known that we can express all of these components in terms of E_y-component or H_y-component, respectively in the TE or TM case. Finally, in these cases of polarization with $e^{i\omega t}$ convention where ω is the circular frequency dependence of the field, we obtain the following equations:

$$\begin{aligned} &\text{TE} : [\partial_z\partial_z + \partial_x\partial_x + k_0^2\varepsilon(x)]E_y = 0 \\ &\text{TM} : [\partial_z(\varepsilon(x))^{-1}\partial_z + \partial_x(\varepsilon(x))^{-1}\partial_x + k_0^2]H_y = 0 \end{aligned} \tag{1}$$

where k_0 is the free-space wave-number, and $\varepsilon(x)$ is the permittivity. ∂_z and ∂_x denote respectively the partial derivative with respect to z and to x.

2.1. Staircase Approximation

In order to reproduce the shape of the tip, we approximate the profile by stair-step. Hence, the tip is discretized using layers as presented in Fig. 2.

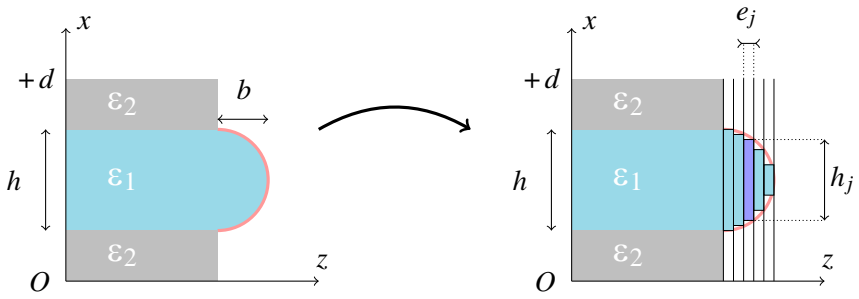

Figure 2. Tip approximation by layers: only one period is depicted.

Each layer is characterized by its thickness e_j, and its permittivity ε_j that spatially depends on the x variable:

$$\varepsilon_j(x) = \begin{cases} \varepsilon_1 = 2, & x \in \left[\dfrac{d-h_j}{2}, \dfrac{d+h_j}{2}\right] \\ \varepsilon_0 = 1, & x \in \left[0, \dfrac{d-h_j}{2}\right] \cup \left[\dfrac{d+h_j}{2}, d\right] \end{cases} \tag{2}$$

2.2. Eigenvalue Problem

Equations (1) can be rewritten concisely introducing the operator L_{Polar}:

$$L_{Polar}\Phi(x,z) = -\frac{1}{k_0^2}\partial_z\Phi(x,z) \tag{3}$$

where $\Phi(x,z)$ represents the y-component of the electric or magnetic field. Since the operator L_{Polar} depends only on the x-variable and since the Fourier Modal Method is based on the series expansion (4), we can use the propagation constant γ and express these components as follows:

$$\Phi(x,z) \approx \sum\nolimits_{m=-M}^{+M} \Phi_m e^{-i\frac{2\pi m x}{d}} e^{-ik_0\gamma z} \tag{4}$$

With this series expansion and using the Fourier factorization rules developed by Li [17, 18], the operators for each polarization are given by:

$$\begin{aligned} L_{TE} &= \|\varepsilon\| - \frac{[\alpha][\alpha]}{k_0^2} \\ L_{TM} &= \|\widetilde{\varepsilon}\|^{-1} \times \left([Id] - \frac{[\alpha]\,\|\varepsilon\|^{-1}\,[\alpha]}{k_0^2}\right) \end{aligned} \tag{5}$$

where $\|\varepsilon\|$ and $\|\widetilde{\varepsilon}\|$ stand for the Toeplitz matrix, respectively, of the Fourier coefficients of the permittivity and of its inverse. $[Id]$ is an identity matrix, $[\alpha]$ is a diagonal matrix whose coefficients are given respectively by $\alpha_p = \frac{2\pi p}{d}$, where $p \in [-M, M]$. The eigenvalues are given by $[\gamma_n]^2$ where $n \in [1, 2M+1]$ and correspond to the effective index of the modes.

For each slice of the tip, the fields can be obtained by a linear combination of the eigenvectors. We remind that each boundary condition is linked by scattering matrices and layer scattering matrices. Then, the global field is reconstructed using the field in each slice (for more information see [19]).

2.3. Perfectly Matched Layers to Study an Aperiodic Structure

We remind that our goal is to model a single waveguide structure (Fig. 1(a)) using a modified version of the classical FMM. To study a non-periodic structure, we introduce perfectly matched layers (PML) which allow to reduce to a single cell. This concept was first introduced and applied

by Bérenger [20]. Among the different formulations of PML, we have chosen the complex coordinate stretching characterized by the parameter $\eta \in [0, 1]$:

$$x^1 = \int_0^x s(x')dx' \text{ where } \begin{cases} s(x) = 1 - \eta i, & x \in D_{PML} \\ s(x) = 1, & x \notin D_{PML} \end{cases} \tag{6}$$

where $D_{PML} = [-\frac{d}{2}, -\frac{d-l_{pml}}{2}] \cup [\frac{d-l_{pml}}{2}, \frac{d}{2}]$ with l_{pml} that corresponds to the thickness of the PML.

We choose to express Maxwell's equations in covariant form in order to easily manage PML. The relation between cartesian coordinates (x, y, z) and new coordinates (x^1, x^2, x^3) is given by:

$$\begin{cases} x^1 = \int_0^x s(x')dx' \\ x^2 = y \\ x^3 = z \end{cases} \tag{7}$$

The tensor $(\sqrt{g}g^{lm})$ for this change of coordinates is [21]:

$$\left(\sqrt{g}g^{lm}\right) = \begin{pmatrix} \frac{1}{s} & 0 & 0 \\ 0 & s & 0 \\ 0 & 0 & s \end{pmatrix} \tag{8}$$

To obtain the new operators, we use Equation (5), with the following modification: $[\alpha]$ is replaced by $\|s\|^{-1}[\alpha]$, where $\|s\|$ stands for the Toeplitz matrix of the Fourier coefficients of the complex coordinate stretching detailed in Equation (6).

3. CONVERGENCE AND VALIDATION WITH INTEGRAL METHOD FOR THE ELLIPTICAL TIP

3.1. Convergence

First of all, we report the convergence of the Aperiodic Fourier Modal Method for the semi-elliptical tip with $b = 4\lambda$ and $h = 3\lambda$ with $\lambda = 1\,\text{cm}$. For this, we vary the two parameters (M, N) where M is associated with the number of terms of Fourier series (4), and N is the number of layers used to represent the shape of the tip. The following results, presented in Table 1, correspond to the maximum intensity in the center of the photonic jet, and for easy reading, values are normalized.

Table 1. Convergence for an elliptical tip ($b = 4\lambda,\ h = 3\lambda$) when the waveguide is excited by the fundamental TE_1 mode.

	Numbers of slices (N)				
M	25	50	75	150	200
15	0.7551	0.8874	0.9285	0.9496	0.9732
30	0.7698	0.9026	0.9441	0.9666	0.9917
80	0.7758	0.9093	0.9510	0.9739	0.9995
150	0.7761	0.9096	0.9514	0.9743	1

In Table 1, the reference value has been obtained with large values for M and N. We can see that from ($M = 30$, $N = 75$), the error is around 5%. Considering these results, we can notice that the method seems to have a good convergence, especially if we consider that the elliptical profile must be finely discretized to correctly reproduce the tip profile.

3.2. Validation

In 2012 and then in 2014 Takakura et al. used the Boundary Integral Equation Method (BIEM) to model a waveguide ended by a tip. This well established rigorous method is based on the Green's

formulas, and it requires less computational time than commercial software. The interested reader may find more information in papers [10, 11].

To validate our method, we compare the results provided by A-FMM with those of the BIEM for the optimized elliptical tip. As can be seen from Fig. 3, both methods provide the same results. Similar results are obtained for TM polarization.

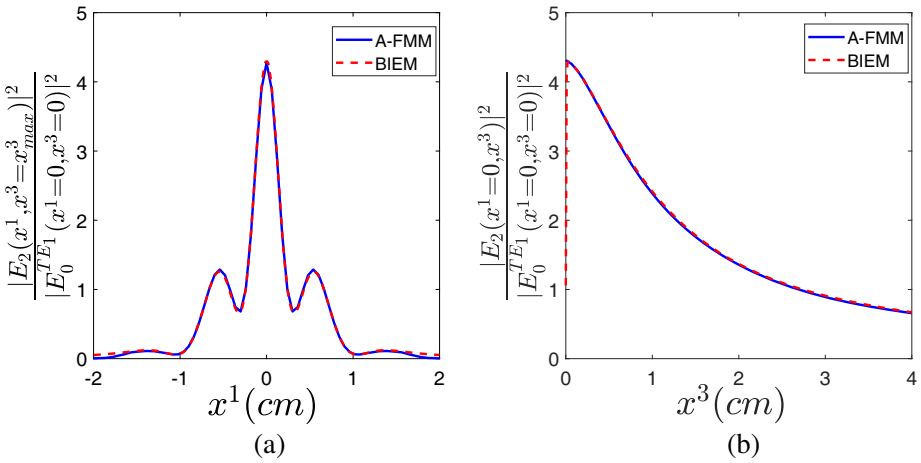

Figure 3. Comparisons between a-FMM method and integral approach results for the elliptical tip ($b = 4\lambda$, $h = 3\lambda$). TE polarization at 30 GHz ($\lambda = 1$ cm). $E_0^{TE_1}$ is the electric field of the fundamental mode in the waveguide and E_2 the x^2-component of the electric field in the air. (a) Cross section at the maximum of the photonic jet ($x^3 = x^3_{\max}$). (b) Longitudinal section of the photonic jet at $x^1 = 0$ cm.

4. OPTIMIZATIONS AND COMPARISONS BETWEEN RECTANGULAR TIP AND ELLIPTICAL TIP

4.1. Numerical Optimization, in *TE* Polarization

Before comparing rectangular and elliptical tip, we want to bring out the best result for both profiles. (Fig. 4).

The computational time being fast, it becomes possible to look for the best result by scanning a large number of parameters of the rectangular or elliptical tip shown in Fig. 4. Our goal is to maximize the intensity of the photonic jet and to minimize the FWHM. In addition, it is necessary to obtain the jet out of the tip. So we decide to maximize the following target function:

$$O_{pt} = \widetilde{\Psi}_{\max} + (1 - \widetilde{x}^3_{\max}) + (1 - \widetilde{F}_W) \tag{9}$$

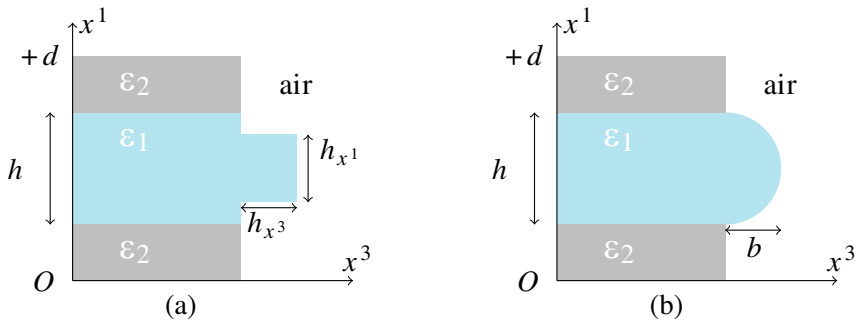

Figure 4. A schematic drawing of a parallel plate waveguide ended with: (a) a rectangular tip or (b) an elliptical tip.

where $\widetilde{\Psi}_{\max}$ is the maximum of the photonic jet normalized by the highest intensity, $\widetilde{x}^3_{\max}$ its position normalized by the greater position, and $\widetilde{F}_W$ the full width at half-maximum (FWHM) normalized by the worst FWHM for the case under consideration.

We specify that some values can be manually removed (enforcing $O_{pt} = 0$) in some cases such as when the maximum of the photonic jet lies inside the structure ($x^3_{\max} \leq 0$).

As can be seen from Fig. 5, the best result for the rectangular tip is given by $h_{x^1} = 1.2\,\text{cm}$, $h_{x^3} = 1.1\,\text{cm}$ which yields $\Psi_{\max}(1.2, 1.1) = 4.54E_0^{TE_1}$ and $F_W(1.2, 1.1) = 0.36\lambda$. For the case of the elliptical profile, the best result is obtained with $b = 4\,\text{cm}$. The electric field maps for the two optimized configurations are shown in Fig. 6.

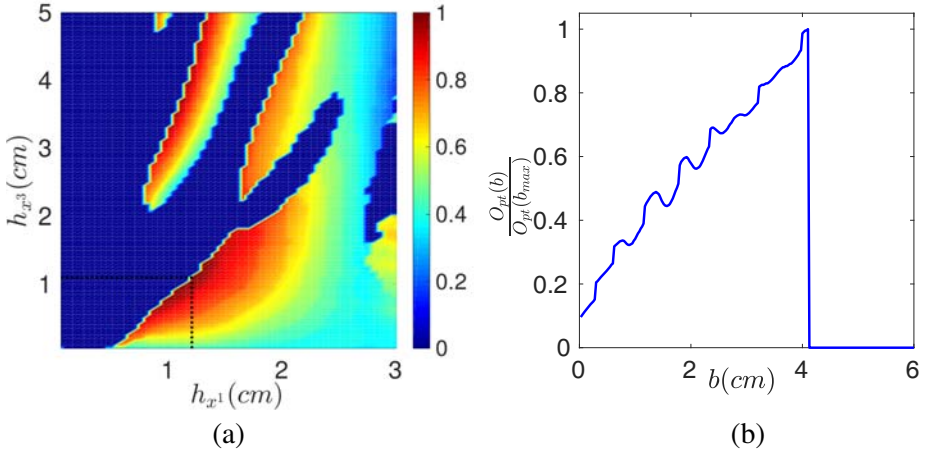

Figure 5. Evolution of the normalized target function O_{pt}. Excitation is done with the fundamental TE mode. (a) Parametric study by varying the two dimensions of the rectangular tip. (b) Parametric study by varying the depth of the elliptical tip.

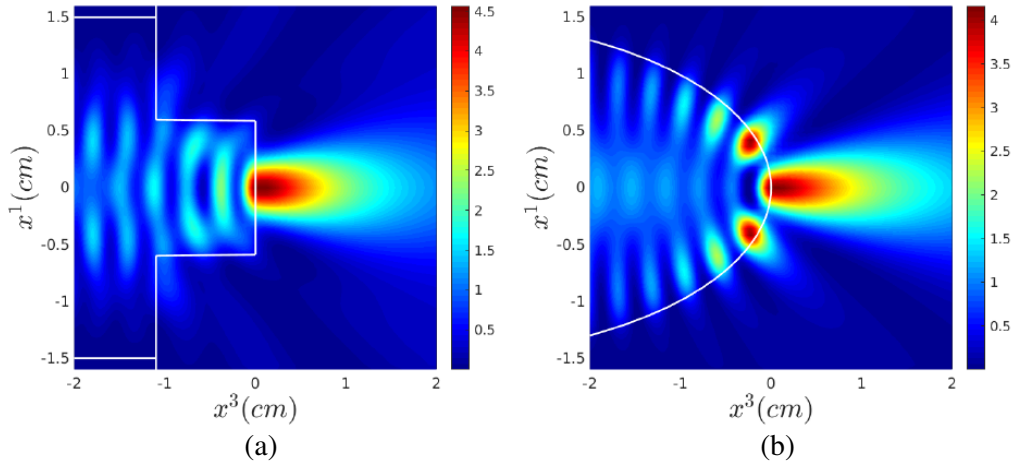

Figure 6. Best numerical results obtained by FMM when $h = 3\lambda$ with $\lambda = 1\,\text{cm}$. (a) The optimized rectangular tip (Fig. 4(a)). (b) The optimized elliptical tip (Fig. 4(b)).

4.2. Elliptical Tip vs Rectangular Tip

The performances of a rectangular tip are compared with those of an elliptical one. Results with no tip are also reported in Table 2. It can be deduced from this table that the optimized rectangular tip improves energy concentrations by 8% and reduces the calculations times by a factor of 10 when we use A-FMM.

Table 2. The planar surface, the optimized elliptical tip and the optimized rectangular tip). The waveguide ($h = 3\lambda$) is excited by the fundamental TE mode ($\lambda = 1\,\text{cm}$). $E_0^{TE_1}$ is the electric field of the fundamental mode in the waveguide.

Tip	Maximum of photonic jet	Calculation time(s)	FWHM (% λ)
Without	1.5 $E_0^{TE_1}(0,0)$	1.04	120
Elliptical	4.2 $E_0^{TE_1}(0,0)$	10.3	28
Rectangular	4.54 $E_0^{TE_1}(0,0)$	1.07	36

From the results of Table 2, we conclude that the rectangular tip offers four advantages:

- A better intensity.
- A simple geometry that makes it easy to manufacture.
- A reduction of the computational time.
- A more compact structure.

It should however be noted that the full-width at half-maximum (FWHM) is slightly degraded, but it is always smaller than one half-wavelength.

5. PROTOTYPE AND EXPERIMENTAL SETUP

To validate these computations, we have compared numerical results with direct observation at microwave frequencies. For that purpose, we have used the same kind of prototypes as in [13].

The structure is composed of a Teflon block ($\varepsilon_r = 2$, $h = 3\,\text{cm}$, $L = l = 20\,\text{cm}$). The Teflon block is sandwiched between two metallic plates creating a dielectric loaded parallel plate waveguide. The tip is fixed using the Teflon screw at the end of the waveguide. The system is excited by a plane wave radiated by a horn antenna located at a sufficient distance to ensure a far-field radiation.

To get maps of electric field in the air, we use a WR28 single-mode rectangular waveguide which will be used as a probe. The rectangular waveguide is connected to the Vectorial Network Analyzer (VNA), and the transmission parameter S_{21} is measured. This scattering parameter is proportional to the electric field parallel to the small side of the WR28 guide. For an overview, we report a photography of the experimental setup (Fig. 7).

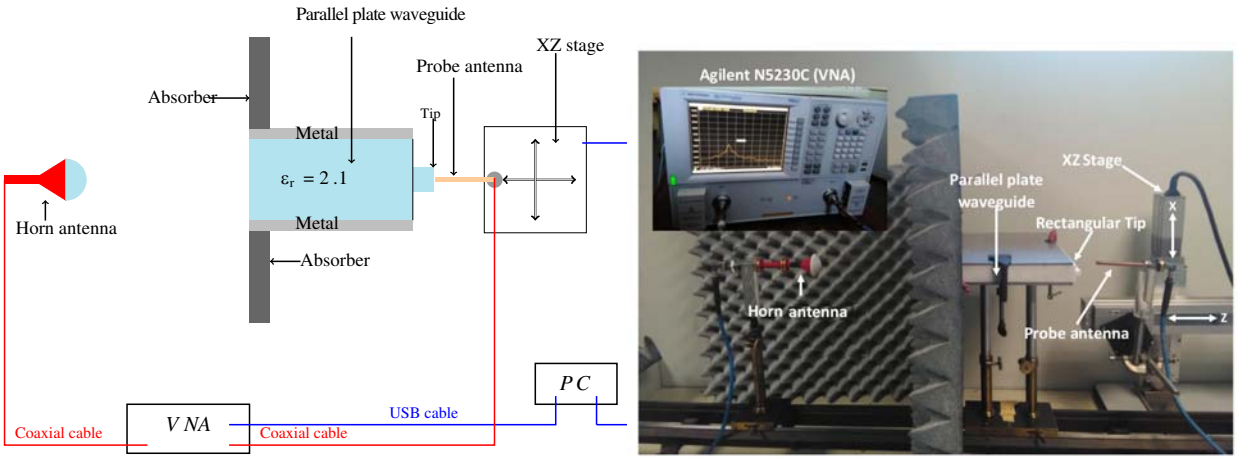

Figure 7. Schematic lateral view and photography of the measuring bench of 2D spatial field mapping system.

For the measurement of scattering parameters, we use a simplified free space calibration method of thru-reflect-match (TRM) type [22]. The main difficulty is in the definition of the thru. We choose to define "thru" by the maximum of the photonic jet before normalization. This leads to the following correction:

$$S_{21_{cor}} = \frac{S_{21_{mes}} - S_{21_{refl}}}{S_{21_{thr}} - S_{21_{refl}}} \tag{10}$$

where $S_{21_{cor}}$ is the transmission obtained after calibration; $S_{21_{mes}}$ is the measurement at each point of the half space under study; $S_{21_{refl}}$ is the measured transmission when a big metallic plate is placed between the source and the probe.

6. NUMERICAL RESULTS VS EXPERIMENTAL OBSERVATIONS

In this part we will compare numerical results with experimental observation for a rectangular tip when $h = 3\lambda$. In the following, in order to move the position of the maximum away from the tip, we have chosen to study the tip with $h_{x^1} = 1\,\text{cm}$ and $h_{x^3} = 0.75\,\text{cm}$.

6.1. *TE* Polarization: The Big Influence of Free Space Excitation

Figure 8(b) shows direct observation of the photonic jet at 30 GHz ($\lambda = 1\,\text{cm}$) produced by the rectangular tip. This result confirms the possibility of generating a photonic jet with a simple rectangular tip. Nevertheless, the current measurement setup uses a plane wave excitation. Comparing Fig. 8(b) with the results obtained with numerical simulation (Fig. 8(a)), it can be noted that they have not exactly the same distribution of energy in the photonic jet.

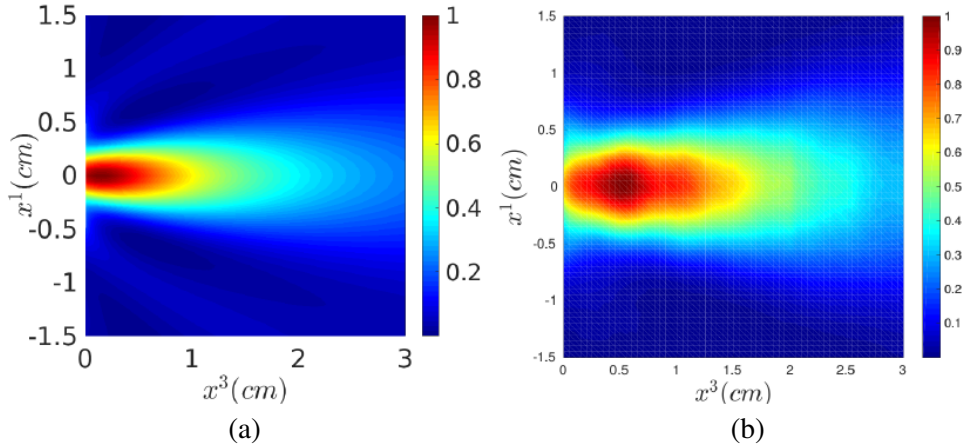

Figure 8. (a) Numerical results obtained by A-FMM for the rectangular tip chosen for the experimental validation $h_{x^1} = 1\,\text{cm}$ and $h_{x^3} = 0.75\,\text{cm}$ when $h = 3\lambda$ with $\lambda = 1\,\text{cm}$ excited by the fundamental mode (TE_1). (b) Measurement of the normalized intensity of electric field, obtained with the free space excitation.

To explore these differences, we plot on Fig. 9 the evolution of the electric field, along the lines extracted from the mapping. On these curves, we have reported measurements and the classical single TE mode excitation, and we have added the computation of our method using a plane wave excitation. As can be seen, the plane wave excites not only the fundamental TE mode but also higher order modes.

These higher order modes have an influence on the position of the center of the jet. They move the position away from the tip. In addition, it can be seen (Fig. 9) that higher modes contribute to the increase of the FWHM (0.36λ to 0.48λ).

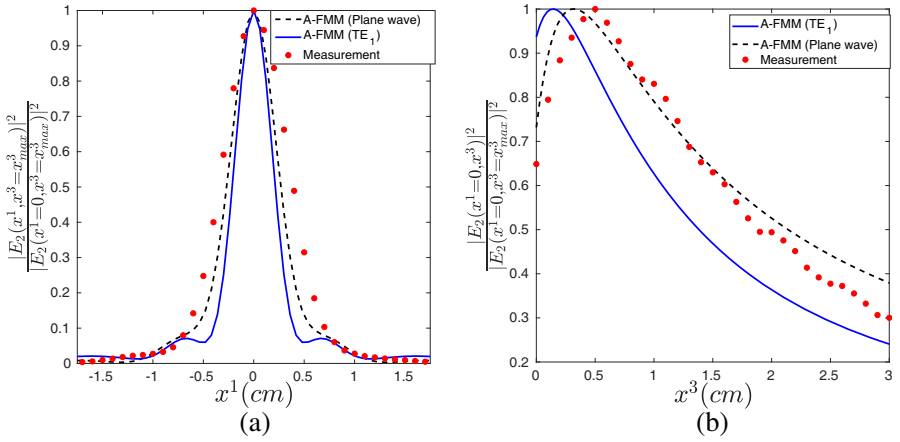

Figure 9. Comparisons for the normalized electric intensity between measurement and simulations. (a) Cross section at the maximum of the photonic jet. (b) Longitudinal section of the photonic jet at $x^1 = 0\,\text{cm}$.

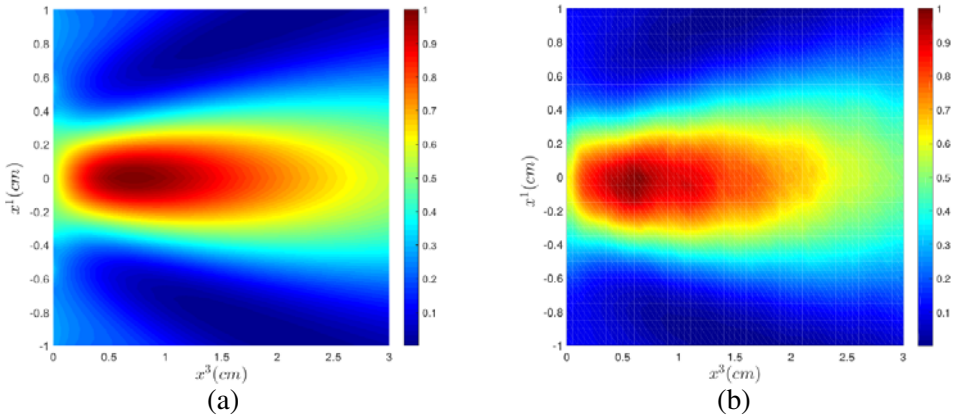

Figure 10. (a) Numerical results obtained by FMM for the rectangular tip ($h_{x^1} = 1\,\text{cm}$ and $h_{x^3} = 0.75\,\text{cm}$) excited by the fundamental mode (TM_0). (b) Measurement of the normalized intensity of electric field at 30 GHz. $h = 3\lambda$ with $\lambda = 1\,\text{cm}$.

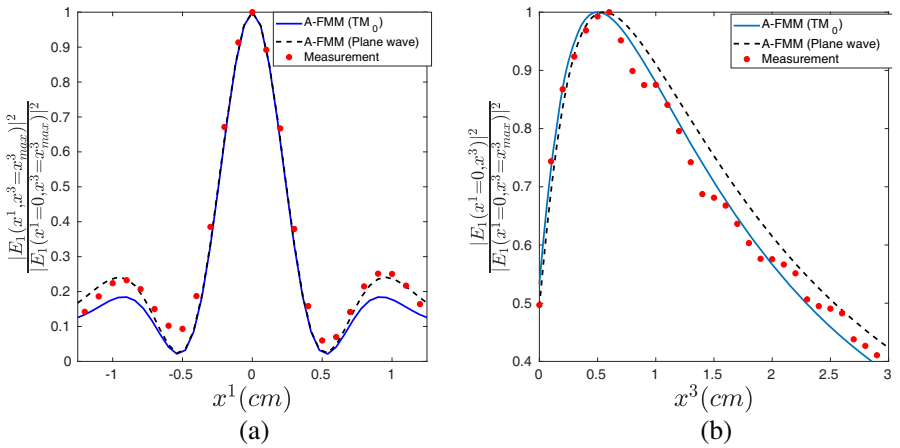

Figure 11. Measurement and simulation results of the normalized electric intensity at 30 GHz for the TM polarization ($h_{x^1} = 1\,\text{cm}$ and $h_{x^3} = 0.75\,\text{cm}$). $h = 3\lambda$. (a) Cross section at the maximum of the photonic jet. (b) Longitudinal section at $x^1 = 0\,\text{cm}$.

6.2. *TM* Polarization: Low Influence of Free Space Excitation

Although optimized for TE polarization, this rectangular tip also produces a photonic jet for the TM polarization ($FWHM = 0.46\lambda$). Unlike the case of TE polarization, differences between single mode excitation and plane wave are very weak (Fig. 10).

To deepen the study of TM polarization, we compare experimental and numerical results of normalized field in Fig. 11. We can see a good agreement between simulated and experimental results. So, we can consider, in this case, that the plane wave excitation predominantly excite the fundamental mode.

7. SUMMARY AND CONCLUSION

We have proposed an aperiodic version of the Fourier Modal Method to study the spatial repartition of the electromagnetic field — also called photonic jet — at the output of a tipped parallel plate waveguide. The developed method is convergent and fast enough to allow optimization investigations. The study on a rectangular tip has shown that the concentration of the jet could be increased by 8%, and that the simplicity of the shape reduces the calculation time by a factor of 10. However, although slightly degraded, the full-width at half-maximum (FWHM) is always less than half a wavelength. To validate these results, a prototype has been realized and measured. The proposed Aperiodic FMM has shown good agreement with measurements, and the importance of a good modelling of the excitation of the waveguide has been demonstrated. Finally, it can be noted that the structure is more sensitive to the excitation in TE polarization than in TM polarization.

ACKNOWLEDGMENT

This project was funded by grants from the Region Auvergne-Rhones-Alpes.

REFERENCES

1. Chen, Z., A. Taflove, and V. Backman, "Photonic nanojet enhancement of backscattering of light by nanoparticles: A potential novel visible-light ultramicroscopy technique," *Opt. Express*, Vol. 12, No. 7, 1214–1220, 2004.
2. Kong, S.-C., A. Sahakian, A. Taflove, and V. Backman, "Photonic nanojet-enabled optical data storage," *Opt. Express*, Vol. 16, No. 18, 13713–13719, 2008.
3. Kong, S.-C., A. V. Sahakian, A. Heifetz, A. Taflove, and V. Backman, "Robust detection of deeply subwavelength pits in simulated optical data-storage disks using photonic jets," *Applied Physics Letters*, Vol. 92, No. 21, 211102, 2008.
4. Itagi, A. V. and W. A. Challener, "Optics of photonic nanojets," *J. Opt. Soc. Am. A*, Vol. 22, No. 12, 2847–2858, Dec. 2005.
5. Lecler, S., Y. Takakura, and P. Meyrueis, "Properties of a three-dimensional photonic jet," *Optics Letters*, Vol. 30, No. 19, 2641–2643, Oct. 2005.
6. Liu, C.-Y., "Photonic jets produced by dielectric micro cuboids," *Appl. Opt.*, Vol. 54, No. 29, 8694–8699, Oct. 2015.
7. Ju, D., H. Pei, Y. Jiang, and X. Sun, "Controllable and enhanced nanojet effects excited by surface plasmon polariton," *Appl. Phys. Lett.*, Vol. 102, No. 171109, 2013.
8. Khaleque, A. and Z. Li, "Tailoring the properties of photonic nanojets by changing the material and geometry of the concentrator," *Progress In Electromagnetics Research Letters*, Vol. 48, 7–13, 2014.
9. Lecler, S., H. Halaq, Y. Takakura, P. Gérard, B. Bayard, S. Robert, and B. Sauviac, "Jet photonique en sortie d'un guide d'onde: De nouvelles perspectives," *(JNOG) Marseille*, Juillet, France, 2011.
10. Takakura, Y., H. Halaq, S. Lecler, S. Robert, and B. Sauviac, "Single and dual photonic jets with tipped waveguides: An integral approach," *IEEE Photonics Technology Letters*, Vol. 24, No. 17, 1516–1518, 2012.

11. Takakura, Y., S. Lecler, B. Ounnas, S. Robert, and B. Sauviac, "Boundary impedance operator to study tipped parallel plate waveguides," *IEEE Photonics Technology Letters*, Vol. 62, No. 11, 5599–5609, 2014.
12. Zelgowski, J., A. Abdurrochman, F. Mermet, P. Pfeiffer, J. Fontaine, and S. Lecler, "Photonic jet subwavelength etching using a shaped optical fiber tip," *Opt. Lett.*, Vol. 41, No. 9, 2073–2076, 2016.
13. Ounnas, B., B. Sauviac, Y. Takakura, S. Lecler, B. Bayard, and S. Robert, "Single and dual photonic jets and corresponding backscattering enhancement with tipped waveguides: Direct observation at microwave frequencies," *IEEE Photonics Technology Letters*, Vol. 63, No. 12, 5612–5618, 2015.
14. Knop, K., "Photonic jet subwavelength etching using a shaped optical fiber tip," *JOSA*, Vol. 68, No. 9, 1206–1210, 1978.
15. Lalanne, P. and G. M. Morris, "Highly improved convergence of the coupled-wave method for TM polarization," *JOSA*, Vol. 13, No. 4, 779–784, 1996.
16. Granet, G. and B. Guizal, "Efficient implementation of the coupled-wave method for metallic lamellar gratings in TM polarization," *JOSA*, Vol. 13, No. 5, 1019–1023, 1996.
17. Li, L., "Fourier modal method," *Gratings: Theory and Numeric Applications*, Evgeny Popov, Aix Marseille Université, 2014.
18. Li, L., "Use of Fourier series in the analysis of discontinuous periodic structures," *JOSA*, Vol. 13, No. 9, 1870–1876, 1996.
19. Granet, G., "Coordinate transformation methods," *Gratings: Theory and Numeric Applications*, Evgeny Popov, Aix Marseille Université, 2014.
20. Berenger, J.-P., "A perfectly matched layer for the absorption of electromagnetic waves," *Journal of Computational Physics*, Vol. 114, No. 2, 185–200, 1994.
21. Plumey, J. P., K. Edee, and G. Granet, "Modal expansion for the 2D Green's function in a non-orthogonal coordinates system," *Progress In Electromagnetics Research*, Vol. 59, 101–112, 2006.
22. Hyani, H., B. Sauviac, K. Edee, G. Granet, S. Robert, and B. Bayard, "Embout multi-guide pour la production de jet photonique appliqué á la détection dans des structures opaques," *JCMM*, France, 2018.